Journal of Traditional and Complementary Medicine 14 (2024) 381–390

Contents lists available at ScienceDirect

Journal of Traditional and Complementary Medicine

journal homepage: www.elsevier.com/locate/jtcme

The chemical composition of Diwu YangGan capsule and its potential inhibitory roles on hepatocellular carcinoma by microarray-based transcriptomics

Qingxin Shi [a,1], Jiangcheng He [b,1], Guangya Chen [a], Jinlin Xu [a], Zhaoxiang Zeng [a], Xueyan Zhao [a], Binbin Zhao [c], Xiang Gao [d,e,f], Zhihua Ye [d,e,f], Mingzhong Xiao [d,e,f,*], Hanmin Li [d,e,f,**]

[a] School of Pharmacy, Hubei University of Chinese Medicine, Wuhan, 430065, China
[b] Wuhan Integrated Traditional Chinese and Western Medicine Orthopedic Hospital, Affiliated Hospital of Wuhan Sports University, Wuhan, 430079, China
[c] School of Basic Medicine, Hubei University of Chinese Medicine, Wuhan, 430065, China
[d] Institute of Liver Diseases, Hubei Key Laboratory of the Theory and Application Research of Liver and Kidney in Traditional Chinese Medicine, Hubei Provincial Hospital of Traditional Chinese Medicine, Wuhan, 430061, China
[e] Affiliated Hospital of Hubei University of Chinese Medicine, Wuhan, 430074, China
[f] Hubei Province Academy of Traditional Chinese Medicine, Wuhan, 430074, China

ARTICLE INFO

Keywords:
Hepatocellular carcinoma
Diwu YangGan
Microarray analysis
LC-MS
Signaling pathways

ABSTRACT

The Traditional Chinese Medicine compound preparation known as Diwu Yanggan capsule (DWYG) can effectively hinder the onset and progression of hepatocellular carcinoma (HCC), which is recognized worldwide as a significant contributor to fatalities associated with cancer. Nevertheless, the precise mechanisms implicated have remained ambiguous. In present study, the model of HCC was set up by the 2-acetylaminofluorene (2-AAF)/partial hepatectomy (PH) in rats. To confirm the differentially expressed genes (DEGs) identified in the microarray analysis, real-time quantitative reverse transcription PCR (qRT-PCR) was conducted. In the meantime, the liquid chromatography-quadrupole time of flight mass spectrometry (LC-QTOF-MS/MS) was employed to characterize the component profile of DWYG. Consequently, the DWYG treatment exhibited the ability to reverse 51 variation genes induced by 2-AAF/PH. Additionally, there was an overlap of 54 variation genes between the normal and model groups. Upon conducting RT-qPCR analysis, it was observed that the expression levels of all genes were increased by 2-AAF/PH and subsequently reversed after DWYG treatment. Notably, the fold change of expression levels for all genes was below 0.5, with 3 genes falling below 0.25. Moreover, an investigation was conducted to determine the signaling pathway that was activated/inhibited in the HCC group and subsequently reversed in the DWYG group. Moreover, the component profile of DWYG encompassed a comprehensive compilation of 206 compounds that were identified or characterized. The findings of this study elucidated the potential alleviative mechanisms of DWYG in the context of HCC, thereby holding significant implications for its future clinical utilization and widespread adoption.

Abbreviations: HCC, hepatocellular carcinoma; DWYG, Diwu Yanggan capsule; 2-AAF, 2-acetylaminofluorene; PH, partial hepatectomy; ALT, alanine transaminase; AST, aspartate aminotransferase; γ-GT, gamma-glutamyl transpeptidase; DEGs, differentially expressed genes; KEGG, Kyoto Encyclopedia of Genes and Genomes; LC-QTOF-MS/MS, liquid chromatography-quadrupole time of flight mass spectrometry; SLPI, secretory leukocyte protease inhibitor.

Peer review under responsibility of The Center for Food and Biomolecules, National Taiwan University.

* Corresponding author. Institute of Liver Diseases, Hubei Key Laboratory of the Theory and Application Research of Liver and Kidney in Traditional Chinese Medicine, Hubei Provincial Hospital of Traditional Chinese Medicine, Wuhan, 430061, China.

** Corresponding author. Institute of Liver Diseases, Hubei Key Laboratory of the Theory and Application Research of Liver and Kidney in Traditional Chinese Medicine, Hubei Provincial Hospital of Traditional Chinese Medicine, Wuhan, 430061, China.

E-mail addresses: xiaomingzhong@hbhtcm.com (M. Xiao), lihanmin69@126.com (H. Li).

[1] These authors contributed equally to this article.

https://doi.org/10.1016/j.jtcme.2023.12.002
Received 18 July 2023; Received in revised form 28 September 2023; Accepted 24 December 2023
Available online 25 December 2023

1. Introduction

Globally, Hepatocellular carcinoma (HCC) is widely acknowledged as a prominent contributor to cancer cases in both males and females, with statistics showing that it is the fifth and ninth most common cancer cause in the former and latter respectively.[1] The etiology and spread of HCC remain incompletely understood, impeding the development of early detection methods and effective treatment protocols.[2,3] Although surgical resection and liver transplantation show promise as primary treatment methods for HCC, their applications have not yet reached optimal levels and are associated with various side effects for patients.[4,5] Furthermore, the application of molecular techniques in HCC diagnosis has been reported to have limitations. Current therapeutic methods for liver cancer mainly include surgical resection, liver transplantation, local ablation, external radiation, *trans*-arterial therapies, chemotherapy, targeted therapy, and immunotherapy. Liver transplantation, curative surgical resection, percutaneous ethanol injection and radiofrequency ablation are considered curative treatments, while transarterial treatments, are currently recognized as treatments that may prolong survival time. Although the development of targeted therapy and immunotherapy for the treatment of HCC has brought new hope to patients with advanced HCC, the overall efficacy of these therapeutic methods remains dismal. Due to its growing significance, the mRNA-based transcriptomics technology is increasingly utilized for early disease diagnosis, disease progression assessment, and drug therapy.[6–8] In view of the afore mentioned, the search for precise prognosis of mRNA-based molecular signatures and treatment methods for controlling HCC have become crucial.

The prevention and treatment of HCC by herbal medicine has been proven an effective therapeutic strategy.[9] Traditional Chinese medicine is widely embraced worldwide as a form of complementary and alternative healthcare. Chinese herbal medicine has been widely used to treat cancer. In the realm of fundamental research, herbal medicine has exhibited efficacy in diminishing the proliferation, invasion, and metastasis of hepatocellular carcinoma (HCC). Moreover, empirical investigations have substantiated the advantageous impact of herbal medicine on survival rates and overall response rates among patients afflicted with HCC.[10,11] The investigation of bioactive compounds from traditional drug or food plants has always been a topic of interest for traditional and complementary Medicine. Over the past few years, researchers have shown interest in green chemistry to extract bioactive compound using environmentally benign agents such as plants, fruits, flowers, algae, yeasts, bacteria, fungi. Diwu Yanggan capsule (DWYG) is a patent herbal formulation (Patent No: 201210580999.2) permitted for use as a drug by the Hubei Food and Drug Administration after many years of intense research (Grant No. Z20113160).[12] It contains five Chinese herbal medicines, including *Artemisia scoparia* Waldst. & Kit., *Schisandra chinensis (Turcz.)* Baill., *Rehmannia glutinosa* Libosch., *Glycyrrhiza uralensis* Fisch. and *Curcuma longa* L. Previous studies have demonstrated that the DWYG has exhibited hepatoprotective effects and has played significant roles in enhancing immune-modulatory responses, ameliorating liver lesions, promoting liver regeneration, exerting virus-killing activities, and inhibiting HCC growth.[12–15] It has been shown that liver injury caused by an array of factors, can significantly hinder the regenerative effects of mature hepatocytes on liver parenchyma.[16] 2-acetylaminofluorene (2-AAF) exposure results in cell lysis and disrupts other liver functions. These have made the 2-AAF/partial hepatectomy (PH) animal model, the most used in assessing the mechanisms by which medicines exert therapeutic effects.[17–19]

In our previous study, it has been demonstrated that DWYG in L-02 cell cultures can reduce alanine transaminase (ALT), aspartate aminotransferase (AST), and Bax levels and upregulate Bcl-2 expression. Additionally, DWYG may control HCC in 2-AAF/PH rats, possibly by modulating and restoring the liver regeneration microenvironment.[12] However, the comprehensive mechanisms of 2-AAF/PH-induced rat pathogenesis and the pharmacological mechanisms of DWYG is still limited. Therefore, the present study aims to explore the mechanisms by which DWYG regulates hepatic transcriptome in 2-AAF/PH-induced hepatocellular carcinoma in view of enhancing its applications in liver treatment. In addition, a component profile of DWYG based on the high-resolution mass spectrometry was constructed and it might help to understand their mechanism on 2-AAF/PH-induced hepatocellular carcinoma.

2. Materials and methods

2.1. Materials and chemicals

In accordance with previous descriptions,[11] the Hubei Provincial Hospital of Traditional Chinese Medicine prepared the DWYG capsules. 2-AAF was obtained from Sigma-Aldrich (Saint Louis, MO, USA). Fisher Scientific (Fair Lawn, NJ, USA) supplied HPLC-grade methanol, while a Millipore water system (Bedford, MA, USA) was used to produce deionized water. An analytical grade formic acid was purchased from Sinopharm Chemical Reagent Co., Ltd (Shanghai, China). The remaining reagents used in this study were purchased from Sinopharm Chemical Reagent Co., Ltd (Shanghai, China).

2.2. Animals and experimental design

48 male Wistar rats (180 ± 10 g) that were Specific-pathogen-free were bought from Hubei Province Experimental Animal Research Center. The rodents were kept in regulated environmental settings, maintaining a temperature of 21 ± 2 °C and a light/dark cycle lasting for 12 h. The experimental protocol was approved by the Institutional Animal Care and Use Committee of the Hubei University of Chinese Medicine (No.202107002).

The modeling of 2-AAF/PH was modified based on previous reports.[20] After one week of acclimatization, the rats were divided into three groups: normal, model, and DWYG groups. Each group consisted of sixteen rats. For the model and DWYG groups, the rats underwent partial hepatectomy and then orally administered a daily dose of 20 mg kg^{-1} 2-AAF for one week. The DWYG capsules were suspended with distilled water in a solution with a concentration of 36 mg mL^{-1}. The rats of DWYG group were given 10 mL kg^{-1}·body $weight^{-1}$·day^{-1} of DWYG solution orally. The rats in normal and model group were given distilled water orally at a dose of 10 mL kg^{-1}·body $weight^{-1}$·day^{-1}. Each group followed this regimen for one week. After receiving the last dose, the rats fasted for 12 h. On the 8th day, rats were anesthetized with a 2 % sodium pentobarbital intraperitoneal injection, and blood samples and liver tissues were gathered. The collected samples were then stored at −80 °C for microarray data analysis.

2.3. Assessment of liver function

The serum levels of AST, ALT and gamma-glutamyl transpeptidase (γ-GT) were assessed as indicators of liver tumor progression[16] and detected according to the kit instructions. The blood specimen underwent centrifugation at a rate of 1700×*g* utilizing a Beckman Coulter GS-6R centrifuge situated in Fullerton, USA, at a temperature of 4 °C for a period of 30 min. Afterwards, the levels of AST, ALT, and γ-GT were measured using a Roche Cobas 8000 modular analyzer, a Cobas-e601 automatic biochemical analyzer produced by Roche Diagnostics in Switzerland. The liver tissues collected from the animals were stored in a solution of formalin (10 % concentration) for further examination of histopathology.

2.4. Microarray hybridization and microarray data analysis

According to kit instructions, total RNA was isolated from hepatic tissues using RNA isolation kit (Tiangen, China). RNA labeling and array hybridization were performed according to the One-Color Microarray-

Based Gene Expression Analysis protocol (Agilent Technology) with minor modifications. An mRNA isolation kit (mRNA-ONLY Eukaryotic mRNA Isolation Kit, Epicentre) was used to remove rRNA from total RNA. After amplifying and trancribing each sample, fluorescent cRNA was generated by random priming methods (Arraystar Flash RNA Labeling Kit, Arraystar). The labeled cRNAs were purified by RNeasy Mini Kit (Qiagen). By using NanoDrop's ND-1000, the specific activity and concentration of the labeled cRNAs were determined. Each labeled cRNA of 1 μg was fragmented by adding 5 μL 10 × Blocking Agent and 1 μL of 25 × Fragmentation Buffer, then heated the mixture at 60 °C for 30 min. Finally, 25 μL 2 × GE Hybridization buffer was added to dilute the labeled cRNA. Assembled to the expression microarray slide, a hybridization solution of 50 μL were dispensed into the gasket slide. A Hybridization Oven (G2545a) from Agilent was used to incubate the slides at 65 °C for 17 h. DNA Microarray Scanner (G2505C) from Agilent was used to scan the hybridized arrays after washing, fixing, and scanning.

Gene expression ratios were determined. Genes with $p < 0.05$ and $|\log2 \text{(Fold Change)}| > 2$ were assigned as differentially expressed genes (DEGs). KOBAS software was used to identify DEGs in the Kyoto Encyclopedia of Genes and Genomes (KEGG) pathway by a two-tailed Fisher's exact test. The pathway with a corrected p value < 0.05 was considered significant. DEGs were visualized by a heat map using the heatmap2 function from the gplots R-package.

2.5. Real-time quantitative reverse transcription PCR

To validate the DEGs from the microarray step, qRT-PCR analysis was performed. Several overlapped DEGs between the model and normal groups, DWYG and model groups comparisons were selected for analysis by qRT-PCR. Total RNA was extracted as described in section 2.3, and 500 ng RNA was reverse transcribed into first-strand cDNA using a Revert Aid First Strand cDNA Synthesis Kit (Thermo, USA). DEG amplifications were conducted by the FastStart Universal SYBR Green Master (Roche, USA) and specific primers (produced by Qing Ke, China) on a LightCycler480 II System (Roche, USA). Primers were designed using high-throughput primer design software according to the predicted sequence of the gene. The primer sequences were shown in Table S1. Ct values were determined as previously described[21] and the ΔΔCt method was used to determine the relative expression levels of target genes and the endogenous housekeeping gene GAPDH was used as an internal standard.

2.6. LC-QTOF-MS/MS analysis

After adding 100 mg of DWYG powder to 5 mL of 75 % methanol in water, the mixture was vigorously vortexed for 5 min and then sonicated for 10 min. After being spun at a speed of 4000 revolutions per minute for a duration of 10 min, the solution was subjected to centrifugation and the resulting liquid, known as the extract, was meticulously extracted.

With the ACQUITY UPLC M-Class system (Waters, Mass. USA), a Waters ACQUITY UPLC BEH C18 column (100 × 2.1 mm, 1.7 μm) from the USA was utilized with a flow rate of 0.3 mL min^{-1}. A total of 2.0 μL was injected. The water/formic acid (1000 1, V/V) was used as mobile phase A, while methanol served as mobile phase B. A binary gradient with linear interpolation was employed as follows: 0.01 min, 10 % B; 15min, 55 % B; 35min, 90 % B; 40min, 98 % B; 45min, 98 % B; 46min,10 % B; 50min, 10 % B.

Mass spectrometric analyses were conducted using a Waters Xevo G2-XS QTof system (Waters, Mass., U.S.A.) equipped with an electrospray ionization source. Positive and negative ion electrospray data acquisition modes were utilized to conduct data analysis. It was determined that the following parameters were most optimal: the source temperature of 100 °C, the desolvation temperature of 500 °C, the cone gas flow of 50 L h^{-1}, the desolvation gas flow of 600 L h^{-1}, the cone voltage of 60 V, and the capillary voltage of 3 kV. For the full scan, the mass ranges were set at m/z 50–1500 Da with scan duration of 1 s. The LockSpray was used to ensure accuracy and reproducibility of all analyses Data were collected in the MS^E continuum mode and were analyzed by MassLynx v4.1 Software (Waters, Mass., U.S.A.).

3. Results

3.1. Liver function analysis

As shown in Table 1, significant (P<0.01) increases in AST, ALT and γ-GT were observed in serum from the 2-AAF/PH induced model group when compared with the control group. The rats treated with the DWYG resulted in 15.1 %, 22.5 % and 35.2 % reductions in the serum levels of AST, ALT and γ-GT activity, respectively, as compared with those from model group (all P<0.05).

3.2. Differential expression analysis

To investigate the underlying mechanisms of DWYG on HCC in 2-AAF/PH rats, transcriptional changes in the liver were studied using microarray protocol. DEGs were characterized using two comparisons: normal and model groups, DWYG and model groups. As shown in Fig. 1, there were 4935 DEGs between the normal and model groups, including 4166 up-regulation genes and 769 down-regulation genes. Moreover, a grand total of 827 DEGs were identified between the DWYG and model groups, with 255 genes exhibiting up-regulation and 472 genes showing down-regulation.

3.3. KEGG pathway enrichment analysis

To analyze the DEGs from the biological pathway insight, DEGs were mapped into the KEGG database record. The KEGG pathway enrichment analysis and the top 20 up-regulated and down-regulated signaling pathways shared by DEGs were shown in Fig. 2.

In these pathways, chemokine signaling pathway, endocytosis, HTLV-1 infection, metabolic pathways, pathway in cancer, PI3K-Akt signaling pathway, Rap1 signaling pathway, and regulation of actin cytoskeleton were among the up-regulated pathways in the model/normal comparison and down-regulated in the DWYG/model comparison, suggesting that although these pathways were induced by 2-AAF/PH, they could be partially reversed by DWYG treatment. In addition, hepatitis B and pathways in cancer were among the down-regulated pathways in the model/normal comparison and up-regulated in the DWYG/model comparison. The pathways in cancer were enriched both in up-regulated and down-regulated of the model/normal comparison and DWYG/model comparison, indicating that there were a large number of targets were involved in this pathway by modeling and the treatment with DWYG. Similarly, the PI3K-Akt signaling pathway was considered as a critical pathway in HCC.

3.4. DEGs related to 2-AAF/PH and DWYG

To identify DEGs whose expression levels were reversed or resistant to DWYG, the Venn diagrams between the model/normal and DWYG/

Table 1
Effect of DWYG on 2-AAF/PH induced hepatocellular carcinoma in activities of AST, ALT, and γ-GT in rats (U/L, mean ± S.D., n = 16).

Group	AST	ALT	γ-GT
Control	121.80 ± 3.51	52.53 ± 0.81	7.05 ± 0.61
Model	175.31 ± 12.71**	89.10 ± 5.86**	29.50 ± 6.57**
DWYG	148.84 ± 9.81##	69.00 ± 6.76##	19.10 ± 3.82#

**p<0.01, compared with the control group.
#p<0.05.
##p<0.01, compared with the model group.

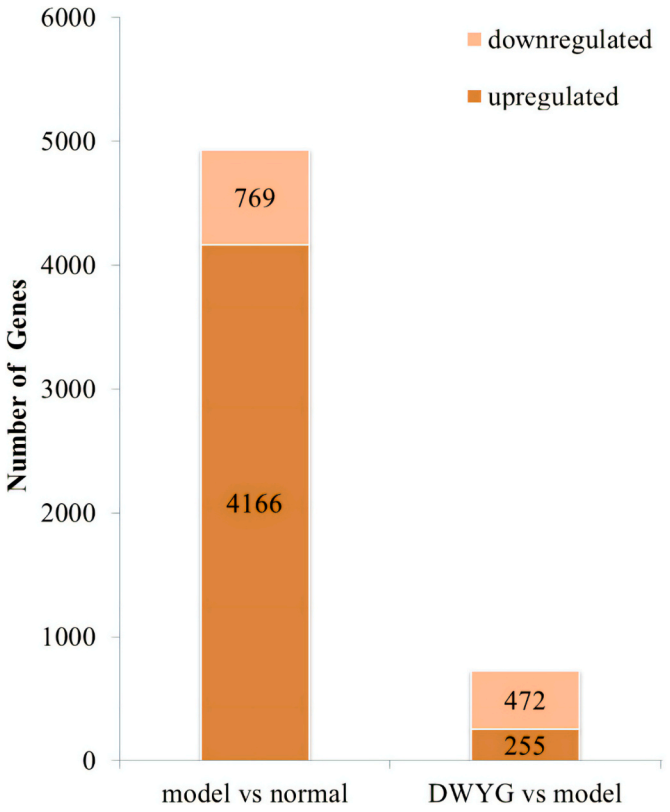

Fig. 1. The number of up-regulated and down-regulated genes in the model/normal and the DWYG/model comparisons.

model comparisons were both performed by selecting the genes of 4-fold change. After DWYG treatment, a total of 54 DEGs were overlapped between the normal/model group and the DWYG/model group (Fig. 3A). As shown in Figs. 3B and 48 of the 54 overlapped DEGs modified by DWYG were up-regulated in the model/normal comparison, whereas these genes were alleviated by the DWYG treatment. In addition, *Ubd, Cyp26a1* and *RT1-S2* genes were down-regulated in the model/normal comparison, while they were up-regulated in the DWYG/model comparison. Besides, 3 genes (*Dock6, Per1* and *Sertad4*) showed no reversions in their expressions between the model/normal and DWYG/model comparisons. These findings implied that DWYG treatment could reverse 51 variation genes induced by 2-AAF/PH.

In order to validate the accuracy of the microarray protocol, genes that were selected for further analysis by qRT-PCR included 2 HCC markers,[22] *Trem2* and *Gpc3*, and a calcium-binding protein and known to promote cell death via glycolysis,[23] *Efhd1*, as well as a regulator of the BMP pathway,[24] *Grem2*, and a therapeutic target of Notch signaling pathway,[25] *Itgb6*, and a kinesin-encoding gene,[26] *Kif12*, which were the overlapped DEGs. As shown in Fig. 4, it was found that the fold change of expression levels among all genes were increased by 2-AAF/PH and reversed after DWYG treatment. In addition, all levels of the fold change of expression levels were below 0.5, among these were 3 genes which were below 0.25. Moreover, the results of microarray showed that these DEGs had similar expression trends when compared to the data of qRT-PCR, suggesting that the results of DEGs was reliable in this study.

3.5. Component profile of DWYG by LC-QTOF-MS/MS

According to the LC retention time, accurate molecular weight and MS/MS behavior, a total of 210 compounds were identified or characterized. Chemical information of 210 compound characterized from DWYG was shown in Table S2. The extracted ion chromatograms of each compound were depicted in Fig. 5. The peaks in Fig. 5 were extracted individually according to the different peak intensities to clearly display all the peaks. Their peak numbers of compounds are consistent with those in Table S2.

The chemical constituents of turmeric mainly were curcuminoids. A total of 82 curcuminoids were identified from Turmeric in this study. The fragmentation patterns of curcumin were fully investigated in previous study.[27,28] One of the characteristic diagnostic ions that can be used to search for the same type of curcuminoids is the product ion at *m/z* 177.0552, which is combined with other product ions produced by various phenyl-substituted groups.

Fifty-six peaks detected in DWYG were identified or characterized as compounds in Licorice. Most of them were flavonoids and six of them were triterpenoids. For instance, liquiritin (compound 137), showed a molecular ion $[M+H]^+$ (*m/z* 419.1310) at 11.60 min (t_R) in positive ion mode. It yielded three prominent fragment ions at *m/z* 257.0797 ($[M + H\text{-Glc}]^+$), 229.0881 ($[M + H\text{-Glc-CO}]^+$), 137.0243 ($[M + H\text{-Glc-}C_8H_8O]^+$). Glycyrrhizin (compound 107) was also detected in positive ion mode at 22.65 min (t_R). It showed a molecular ion $[M+H]^+$ at *m/z* 823.4088 ($C_{42}H_{62}O_{16}$). The production of ions at *m/z* 647.3810 ($[M + H\text{-Glc}]^+$), 471.3462 ($[M + H\text{-2Glc}]^+$), 453.3364 ($[M + H\text{-2Glc-}H_2O]^+$). These two compounds of retention time were confirmed by comparison with reference substances.

A total of 15 compounds, including flavanones, coumarins and organic acid were detected in *Artemisia capillaris*. Arcapillin (compound 142), showed an accurate mass at *m/z 361.0941* in positive ion mode, corresponding to the molecular formula $C_{18}H_{16}O_8$. The ion at *m/z* 347.0714 was produced through losing the CH_3 group. Ion at *m/z* 333.0970 was formed by loss of CO from the parent ion. Ion at *m/z* 197.0476 was generated by elimination of $C_9H_8O_3$ from the parent ion.

Forty-three compounds were detected in *Schisandra chinensis*. For example, Schisandrin (compound 154) was detected at 17.97 min (t_R) in positive ion mode. It showed molecular ions $[M+H]^+$ at *m/z* 433.2193 ($C_{24}H_{32}O_7$) and $[M+Na]^+$ at *m/z* 455.2076. The MS/MS fragmentation of *m/z* 433.2193 exhibited a series of major product ions at *m/z* 415.2108 $[M + H\text{–}H_2O]^+$, 385.1989 $[M + H\text{–}H_2O\text{–OMe}]^+$ and 361.1617 $[M + H\text{–}H_2O\text{–}C_4H_6]^+$.

In this study, 4 compounds were detected in *Rehmanniae Radix Preparata* as shown in Table S2. All of them existed mainly in $[M+Na]^+$ form. For instance, Rehmannioside D (compound 209), showed a molecular ion $[M+Na]^+$ (*m/z* 709.2172) at 0.98 min (t_R) in positive ion mode. The main fragment ions at *m/z* 669.2244, 527.1592, 365.1065, and 203.0505 of Rehmannioside D were observed. Furthermore, polysaccharides, the other major constituents of *Rehmanniae Radix Preparata*, were not detected in the existing detecting conditions because of their poor ionization efficiency in mass spectrometry.

4. Discussions

The present study uses microarrays to investigates how DWYG treatment can significantly regulate HCC biomarkers in a 2-AAF/PH rat model. The five pathways and 54 overlapped DEGs were screened to be associated with the inhibitory mechanisms of DWYG on HCC. Meanwhile, the component profile of DWYG was characterized using liquid chromatography-quadrupole time of flight mass spectrometry (LC-QTOF-MS/MS). As a result, a total of 210 compounds were identified or characterized in DWYG, 10 of which were confirmed by corresponding standards, and the others were characterized by the comparing their MS/MS behavior with that of reported literatures. A further assignment was made to the individual herbs based on the compounds; 4 compounds were from *Rehmanniae Radix Preparata*, 15 were from *Artemisia capillaris*, 43 were from *Schisandra chinensis*, 82 were from Turmeric, and 56 were from Licorice. These findings could provide helpful chemical information for exploring DWYG efficacy and the mechanism of action.

Curcumins and their derivatives have been used widely in preclinical in vitro and in vivo models of hepatocellular carcinoma.[29] Besides the strong content in triterpenoids, such as glycyrrhizin and glycyrrhetinic

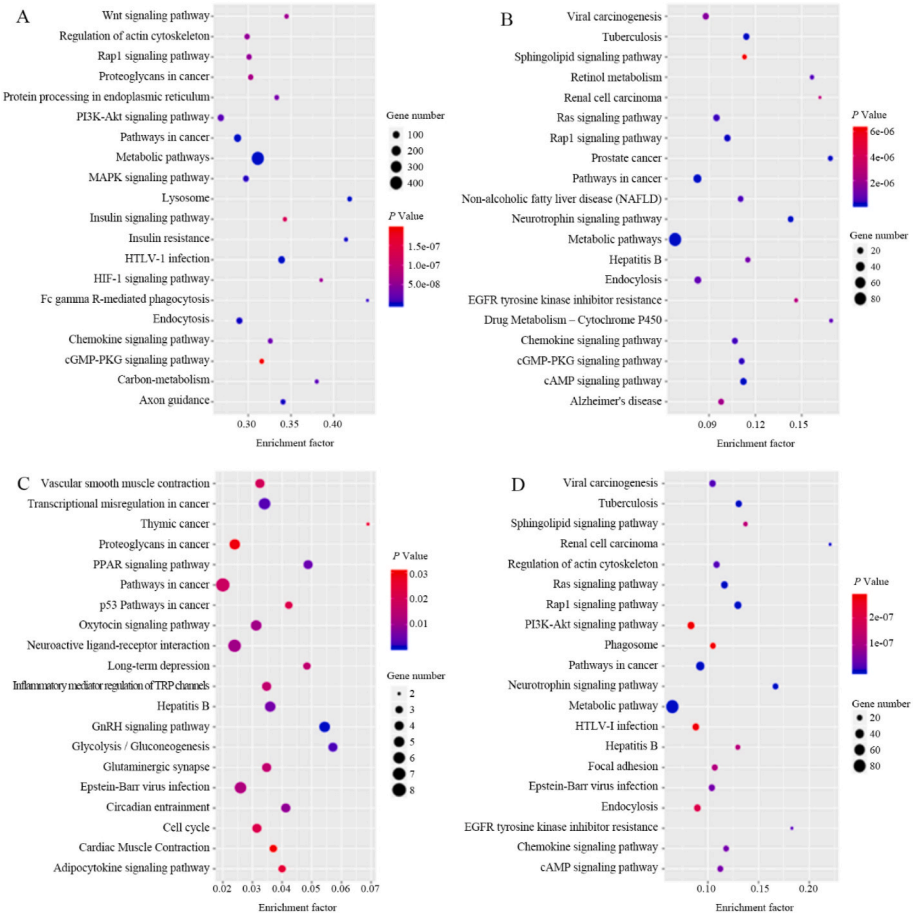

Fig. 2. Bubble diagrams of KEGG pathway enrichment for DEGs in (A) model/normal (up-regulated), (B) model/normal (down-regulated), (C) DWYG/model (up-regulated) and (D) DWYG/model (down-regulated).

acid, was demonstrated to suppress NF-κB activation in TNF-α-induced hepatocytes.[30] Schisandrin A and Schisandrin B could induce *Oatp1b1* expression and increase its transporter activity in the human hepatocellular liver carcinoma cell line.[31] Already basic formulations likely contain ingredients with considerable biological activity. In addition, based on the component profile of DWYG capsule, it is more scientific and reasonable for the study of the spectrum–effect relationship between it and the mechanism of HCC.

It was investigated that DWYG capsule has therapeutic effect on CCl4-induced liver injury in vivo and in L-02 cells by the regulation of Bax/Bcl-2 signaling pathway.[32] In our previous study,[15] the rat model was used to determine the effect of the DWYG capsule on the occurrence and development of liver cancer and to explore its mechanisms on the development and progression of liver cancer. The hepatoprotective effects of DWYG were investigated and compared with Sorafenib. The results showed that DWYG treatment could improve the liver regeneration microenvironment by regulating the RAF/MEK/ERK pathway, thereby inhibiting the occurrence and development of liver cancer. In another previous study,[15] the clinical results suggest that DWYG could improve the liver histological response rate of patients with hepatitis B e antigen (HBeAg)-negative Chronic hepatitis B virus (CHB). Specifically, it has a stable long-term curative effect and can significantly reduce the incidence of liver cirrhosis. In addition to using antiviral drugs, treating HBeAg-negative CHB with DWYG is also an important way to improve the clinical effect by influencing host factors, which provides a reference for further research and clinical applications.

Chemokine signaling pathway regulated HCC pro-inflammatory which could lead to hepatobiliary cancer, characterized by swollen hepatic tissues. Both past and recent research concur that the pathways of chemokines have a crucial impact on the creation of a tumor-promoting microenvironment and the advancement of hepatobiliary cancer.[33,34] Chemokines and their receptors play a crucial role in the migration of leukocytes and cancer cells, being linked to tumors at every stage of cancer growth and serving as important factors in tumor advancement. Chemokines play a crucial role in the immune response by interacting with different receptors to regulate the movement of immune cells.[35] CX3CL1, a chemokine and adhesion molecule expressed by vascular endothelial cells.[36] CX3CL1 could convert inflammatory Ly6C^{high} macrophages into reparative Ly6C^{low} macrophages. Restorative Ly6C^{low} not only display anti-inflammatory and tissue-protective characteristics but also facilitate liver tissue injury repair and ultimately impede the advancement of liver fibrosis.[37] Licorice extract was discovered to inhibit the expression of chemokine mRNA induced by TNF-alpha, in a manner that depended on the dosage.[38] TREM2 is a member of the receptor family with a single IgV domain, found on the surface of myeloid cells as transmembrane glycoproteins. Upon activation of TREM2, the cell surface exhibits expression of the chemokine receptor CCR7, thereby facilitating chemokine-directed migration towards chemokine receptor ligands. One further article has reported that the curcumin could regulate the TREM2, alleviating apoptosis.[39] The secretory leukocyte protease inhibitor (SLPI) is a protein that belongs to the whey acidic protein four-disulfide core family. It is a non-glycosylated, single-chain protease inhibitor. SLPI's primary role is to hinder antimicrobial activity, regulate inflammation, suppress proteases, and regulate immune response.[40] According to the reported article, SLPI hindered the activation of NF-κB, thereby suppressing the production of chemokines in response to microbial signals.[41] During our investigation, we observed an up-regulation of the *Cx3cl1*, *Trem2*, and *Slpi* genes in the

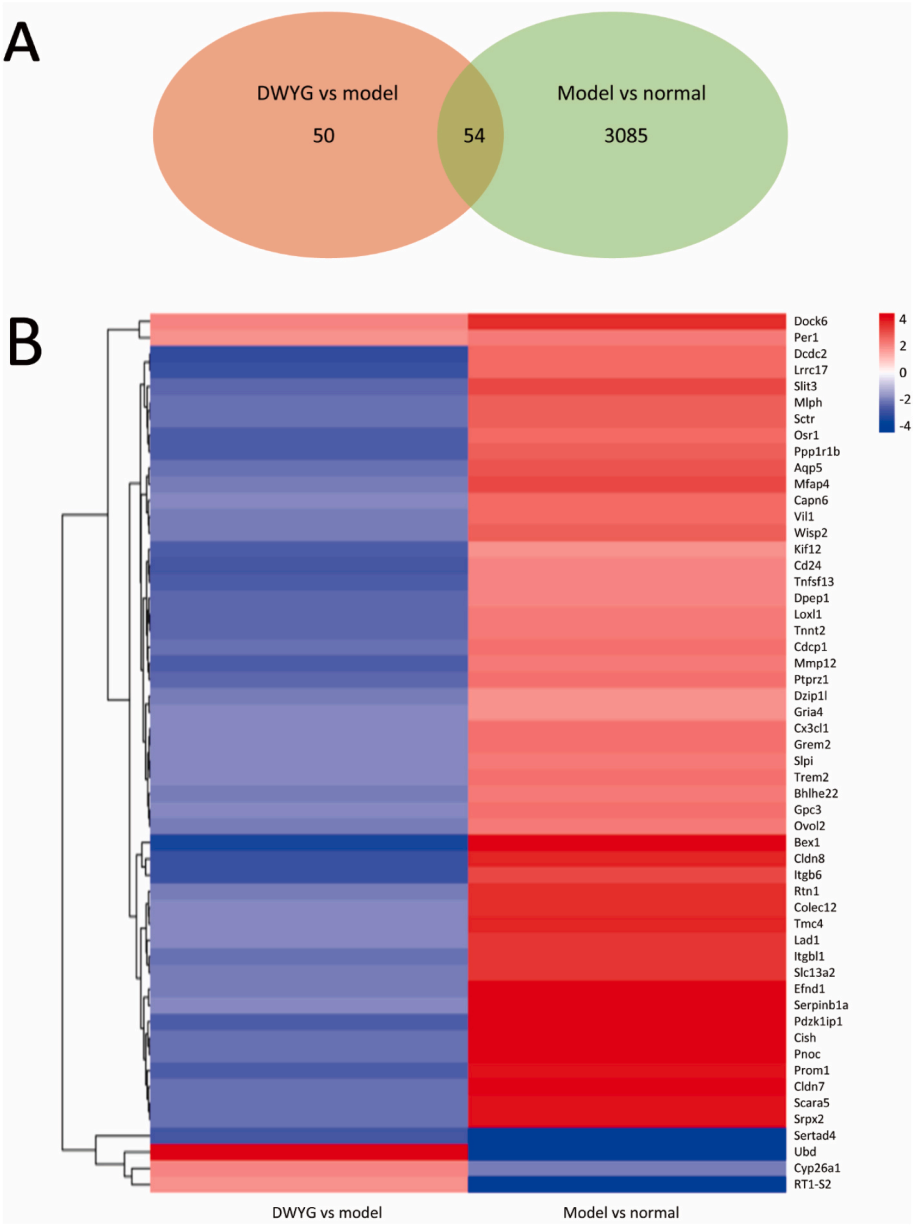

Fig. 3. DWYG and 2-AAF/PH affect alterations in liver transcription. (A) The Venn diagram shows DEGs common to both the model/normal and DWYG/model genes. (B) Heat maps of the common DEGs between the model/normal and DWYG/model comparisons.

comparison between the model and normal conditions. This result indicated that DWYG could inhibit the progression of hepatobiliary cancer by Chemokine signaling pathway.

The results of the current investigation validate that the PI3K/Akt pathway was up-regulated in the model group. There are several cellular processes that are influenced by the PI3K/Akt pathway, including growth and survival of tumors. The PI3K/Akt pathway has an impact on various cellular processes, such as the development and viability of tumors.[42] Also, PI3K/Akt signaling contributes to tumorigenesis by working in conjunction with mTOR.[43] Some literatures have reported that licorice, turmeric, *Artemisia capillaris, Schisandra chinensis* and *Rehmanniae Radix Preparata* could all inhibition of the PI3K-Akt signaling pathway.[44–48] The lignans of *Schisandra chinensis* has been reported to decrease the PI3K, Akt and Akt downstream signaling molecules Mcl-1 expression.[49] Moreover, a recent study demonstrated that TREM2 functions as a cancer inhibitor in HCC by directing its attention towards the PI3K/Akt/β-catenin pathway.[22] Through its ability to promote cell proliferation, angiogenesis, and inhibit apoptosis, CAPN6 promotes tumor development. Through the PI3K/AKT signaling pathway, CAPN6 is regulated in liver cancer, where it promotes proliferation and inhibits apoptosis.[50] In order to effectively participate in cell migration and adhesion, SRPX2 is composed of cell secretory proteins and polysaccharides.[43] In a prior investigation, it was demonstrated that suppression of SRPX2 effectively blocked the activation of the PI3K/Akt/mTOR pathway in prostate cancer cells.[51] DPEP1, a metalloproteinase that relies on zinc, is commonly disrupted in numerous cancer types. By activating the PI3K/Akt/mTOR signaling pathways, it functioned as an oncogene in hepatoblastoma.[52] However, *Capn6*, *Srpx2* and *Dpep1* were all down-regulated by DWYG in our study. The findings of the present study and indeed the theories put forward in available literature provide an update on the discovery and development of clinical substances that can disrupt HCC pro-inflammatory factors and pathways such as *PI3K* and *Akt* genes.[53]

Proteoglycans play a crucial role in the cellular and pericellular microenvironments, serving as important molecular agents in cancer biology.[54] In our study, *Gpc3*, *Cdcp1*, *Loxl1* and *Ptprz1* genes were

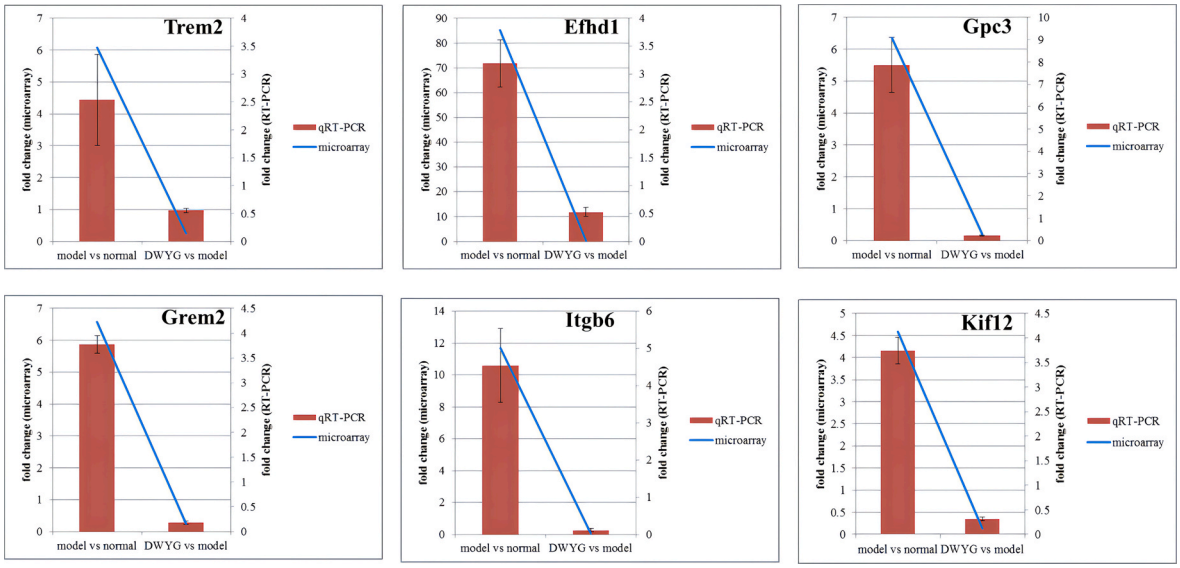

Fig. 4. qRT-PCR validation results of the DNA microarray. Blue line signifies DNA microarray data for the DEGs while the red bar stands for qRT-PCR results for the DEGs. The values were the means of three replicates of three different experiments.

up-regulated in the model/normal comparison, while they were down-regulated in the DWYG/model comparison. Among of these genes, *Gpc3* is a membrane heparan sulfate proteoglycan, is specifically expressed in HCC.[55] The study conducted by Pan, Z. and colleagues has shown that increased expression of *Gpc3*, hinders the onset and progression of HCC.[56] An expressed cell surface glycosylated transmembrane protein, *Cdcp1* could be highly overexpressed in cancers such as HCC. Its overexpression was associated with more aggressive forms of these cancers.[57] Inhibition of *Loxl1* may delay liver fibrosis progression since *Loxl1*is involved in the activation of HSCs during fibrogenesis.[58] *Ptprz1* produces either chondroitin sulfate proteoglycan or a variant lacking proteoglycan in various types of cancer tissues. The various roles it plays in the development, advancement, and spread of cancer also have an impact on the treatment and outlook of the disease.[59]

Pathways in cancer is a series of signal pathways related to cancer, including *Wnt* and *TGF-β* etc. Dysregulation of the Wnt signaling pathway is linked to various types of cancer, such as breast cancer, prostate cancer, liver cancer, and more.[60] PROM1, serving as a cancer stem cell indicator, is a subject of interest in Wnt signaling regenerative pathways in various types of cancer cells. The experiments demonstrated that GPC3 could promote the growth of HCC by stimulating canonical *Wnt* signaling.[61] From the material basis of DWYG, we found that DWYG has great advantages in decrease the *Wnt* signaling pathway. For example, it has been reported that curcumin could inhibits HCC tumor growth by downregulated of *Wnt/β-catenin* signaling pathway.[62,63] Similarly, licorice flavonoids and catalpol could also decrease the *Wnt* signaling pathway. TGF-β is a crucial regulatory cytokine throughout the liver fibrosis progression.[64] Throughout the progression of liver fibrosis, TGF-β plays a vital role as a regulatory cytokine. Currently, TGF-β is recognized as the most potent cytokine in stimulating hepatic fibrosis. It triggers HSC activation via the TGF-β-Smad signaling pathway, leading to enhanced synthesis of ECM in HSCs and modification of ECM metabolism, ultimately facilitating the progression of liver fibrosis. Research has indicated that blocking TGF-β signaling leads to numerous collaborative downstream consequences that are expected to enhance the clinical outcome in HCC.[65] There are studies have demonstrated that the overexpression of *Mfap4* could mitigate the TGF-β-induced enhanced expression of fibrosis-related proteins,[66] and GPC3 could also affects HCC cell growth by TGF-β signaling pathway.[56] Moreover, from the perspective of material fundamental, curcumin could significantly suppressed mRNA expression levels of TGF-β,[67] and glycyrrhizin,[68] catalpol[69] and schisandrin B[70] also have the same function.

The movement of cells plays a crucial role in the invasion and spread of tumors, and controlling this mechanism will pave the way for effective cancer treatments. The actin cytoskeleton plays a crucial role in the movement of tumor cells and their ability to spread to other parts of the body.[71] Recently, it has been reported that adenylate cyclase-associated protein 1, a protein responsible for regulating the actin cytoskeleton, is involved in cell motility and the development of pancreatic cancer.[72] It has been reported that curcumin can inhibit cell migration and invasion, as well as downregulate the expression of the *Cdc42* gene and *Cdc42*-related target genes. Additionally, it caused reorganizations of the actin cytoskeleton.[73]

Although the therapeutic effect of DWYG on HCC has been confirmed based on our previous and current research, its efficacy and safety of DWYG compared to other treatments for HCC remains to be clear. Additionally, the study did not investigate the potential side effects of DWYG, which is considered in our further research. In addition, based on the component profile of DWYG capsule, it is more scientific and reasonable for the study of the spectrum–effect relationship between it and the mechanism of HCC. The manuscript suggests that DWYG may be a promising area for further research and clinical development, and that it may have potential as a complementary or alternative treatment for HCC.

5. Conclusions

The current investigation examined the transcriptomic consequences of DWYG treatment on the inhibition of HCC initiation and progression. Findings demonstrated that DWYG exhibited the ability to restore impaired organ and systemic functions through the modulation of various pathways, including chemokine signaling, endocytosis, HTLV-1 infection, metabolic pathways, pathway in cancer, PI3K-Akt signaling, Rap1 signaling, hepatitis B, and regulation of actin cytoskeleton. Furthermore, DWYG treatment effectively reversed the expression of 51 genes that were altered by 2-AAF/PH induction. Moreover, the component profile of DWYG provides evidence suggesting that these potential mechanisms may be associated with the active components present in the herbal formulation. Subsequent investigations will prioritize exploring the synergistic effects among the constituents in DWYG and their regulatory targets on HCC, potentially leading to advancements in the field of HCC therapy.

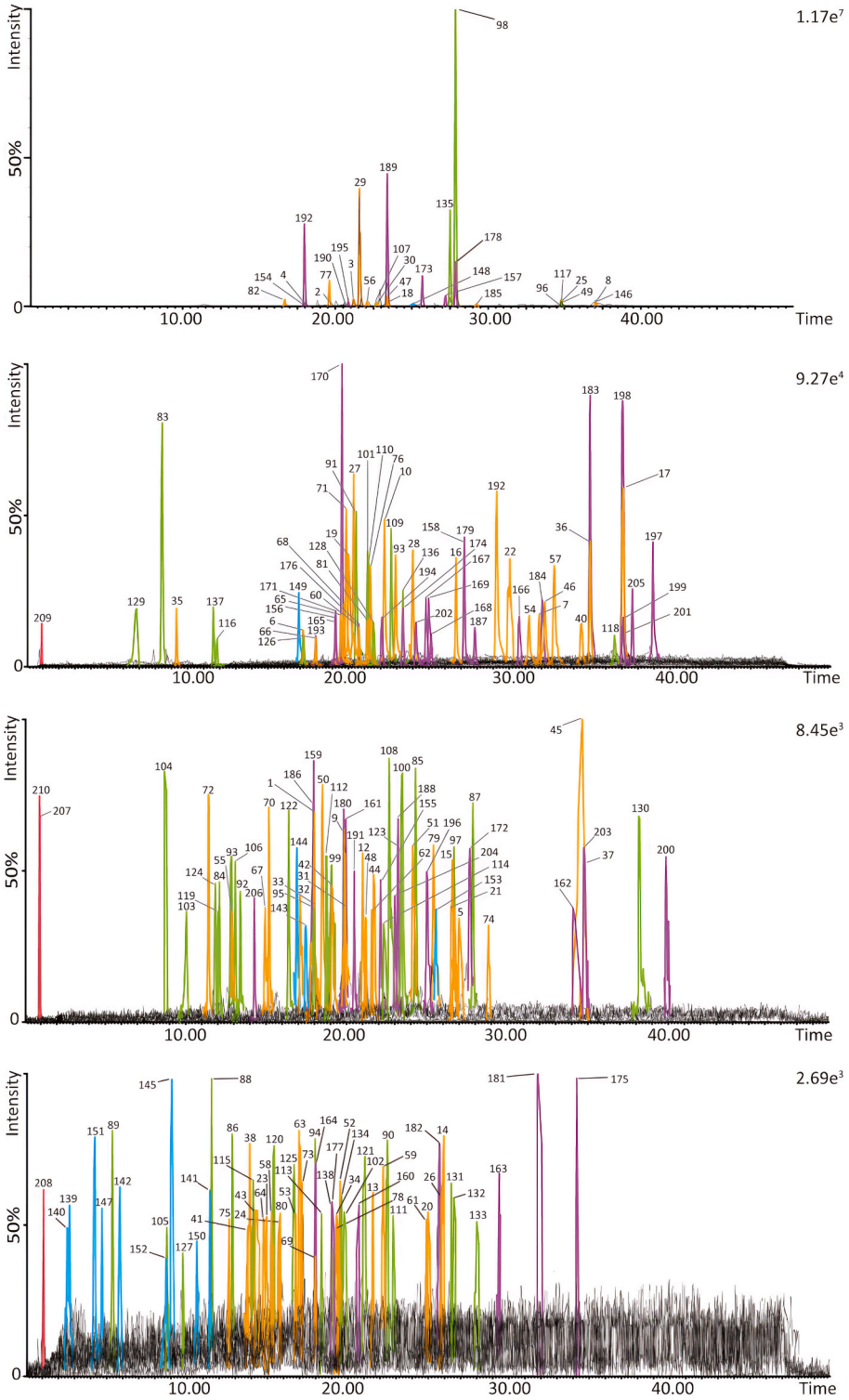

Fig. 5. Extracted ion chromatograms of the 206 compounds characterized from DWYG by LC-QTOF-MS/MS.

Author contributions

All authors contributed to the conception and design of the study. Writing – Original Draft Preparation and Writing – Review & Editing: Qingxin Shi and Jiangcheng He; Methodology and Software Guangya Chen and Jinlin Xu; Formal Analysis, Investigation, and Visualization: Zhaoxiang Zeng, Xueyan Zhao, Binbin Zhao, Xiang Gao and ZhihuaYe; Supervision, Project Administration, and Funding Acquisition: Mingzhong Xiao and Hanmin Li. All authors gave final approval and agreed to be accountable for the aspects of the work.

Funding

This research was funded by the National Natural Science Foundation of China with grant number [No. 81573815, No. 81973669, No. 81703912 and No. 81603484].

Data availability statement

The original contributions presented in the study are included in the article/Supplementary Material; further inquiries could be directed to the corresponding authors.

Declaration of generative AI in scientific writing

The AI tools were not to the used to analyze and draw insights from data as part of the research process.

Declaration of competing interest

None.

Appendix A. Supplementary data

Supplementary data to this article can be found online at https://doi.org/10.1016/j.jtcme.2023.12.002.

References

1. Ferlay J, Soerjomataram I, Dikshit R, et al. Cancer incidence and mortality worldwide: sources, methods and major patterns in GLOBOCAN 2012. *Int J Cancer*. 2015;136(5):E359–E386.
2. Bruix J, Han KH, Gores G, et al. Liver cancer: approaching a personalized care. *J Hepatol*. 2015;62(1 Suppl):S144–S156.
3. He W, Zeng Q, Zheng Y, et al. The role of clinically significant portal hypertension in hepatic resection for hepatocellular carcinoma patients: a propensity score matching analysis. *BMC Cancer*. 2015;15:263.
4. Llovet JM, Bruix J, Gores GJ. Surgical resection versus transplantation for early hepatocellular carcinoma: clues for the best strategy. *Hepatology*. 2000;31(4):1019–1021.
5. Wang L, Abou-Alfa GK, Liu F, et al. Novel methodology of response assessment in hepatocellular carcinoma (HCC) -Assessing response by change in tumor enhancement in distinction from conventional means. *J Clin Oncol*. 2004;22(14_suppl):3107.
6. Haghjoo N, Moeini A, Masoudi-Nejad A. Introducing a panel for early detection of lung adenocarcinoma by using data integration of genomics, epigenomics, transcriptomics and proteomics. *Exp Mol Pathol*. 2020;112, 104360.
7. Bernard V, Semaan A, Huang J, et al. Single-cell transcriptomics of pancreatic cancer precursors demonstrates epithelial and microenvironmental heterogeneity as an early event in neoplastic progression. *Clin Cancer Res*. 2019;25(7):2194–2205.
8. De Bastiani MA, Klamt F. Integrated transcriptomics reveals master regulators of lung adenocarcinoma and novel repositioning of drug candidates. *Cancer Med*. 2019;8(15):6717–6729.
9. Hong M, Li S, Tan HY, et al. Current status of herbal medicines in chronic liver disease therapy: the biological effects, molecular targets and future prospects. *Int J Mol Sci*. 2015;16(12):28705–28745.
10. Zhou Y, Xue R, Wang J, et al. Puerarin inhibits hepatocellular carcinoma invasion and metastasis through miR-21-mediated PTEN/AKT signaling to suppress the epithelial-mesenchymal transition. *Braz J Med Biol Res*. 2020;53(4), e8882.
11. Wang Z, Li J, Ji Y, et al. Traditional herbal medicine: a review of potential of inhibitory hepatocellular carcinoma in basic research and clinical trial. *Evid Based Complement Alternat Med*. 2013;2013, 268963.
12. Zhao BB, Li HM, Gao X, et al. The herbal compound "diwu yanggan" modulates liver regeneration by affecting the hepatic stem cell microenvironment in 2-acetylaminofluorene/partial hepatectomy rats. *Evid Based Complement Alternat Med*. 2015;2015, 468303.
13. Shen X, Cheng S, Peng Y, et al. Attenuation of early liver fibrosis by herbal compound "Diwu Yanggan" through modulating the balance between epithelial-to-mesenchymal transition and mesenchymal-to-epithelial transition. *BMC Compl Alternative Med*. 2014;14:418.
14. Li H, Ye Z, Gao X, et al. Diwu Yanggan capsule improving liver histological response for patients with HBeAg-negative chronic hepatitis B: a randomized controlled clinical trial. *Am J Transl Res*. 2018;10(5):1511–1521.
15. Ye Z, Gao X, Zhao B, et al. Diwu Yanggan capsule inhibits the occurrence and development of liver cancer in the Solt-Farber rat model by regulating the Ras/Raf/Mek/Erk signaling pathway. *Am J Transl Res*. 2018;10(11):3797–3805.
16. Zhou BG, Zhao HM, Lu XY, et al. Erzhi pill(R) repairs experimental liver injury via TSC/mTOR signaling pathway inhibiting excessive apoptosis. *Evid Based Complement Alternat Med*. 2017;2017, 5653643.
17. Sehrawat A, Sultana S. Evaluation of possible mechanisms of protective role of Tamarix gallica against DEN initiated and 2-AAF promoted hepatocarcinogenesis in male Wistar rats. *Life Sci*. 2006;79(15):1456–1465.
18. Bae SH, Oh SH, Yoon SK, et al. Proliferation of hepatic oval cells via cyclooxygenase-2 and extracellular matrix protein signaling during liver regeneration following 2-AAF/partial hepatectomy in rats. *Gut Liver*. 2011;5(3):367–376.
19. Zheng D, Oh SH, Jung Y, et al. Oval cell response in 2-acetylaminofluorene/partial hepatectomy rat is attenuated by short interfering RNA targeted to stromal cell-derived factor-1. *Am J Pathol*. 2006;169(6):2066–2074.
20. Chen L, Zhang W, Liang HF, et al. Activin A induces growth arrest through a SMAD-dependent pathway in hepatic progenitor cells. *Cell Commun Signal*. 2014;12:18.
21. Livak KJ, Schmittgen TD. Analysis of relative gene expression data using real-time quantitative PCR and the 2(-Delta Delta C(T)) Method. *Methods*. 2001;25(4):402–408.
22. Tang W, Lv B, Yang B, et al. TREM2 acts as a tumor suppressor in hepatocellular carcinoma by targeting the PI3K/Akt/beta-catenin pathway. *Oncogenesis*. 2019;8(2):9.
23. Panga V, Kallor AA, Nair A, et al. Mitochondrial dysfunction in rheumatoid arthritis: a comprehensive analysis by integrating gene expression, protein-protein interactions and gene ontology data. *PLoS One*. 2019;14(11), e0224632.
24. Viaene AN, Zhang B, Martinez-Lage M, et al. Transcriptome signatures associated with meningioma progression. *Acta Neuropathol Commun*. 2019;7(1):67.
25. Zhuang H, Zhou Z, Ma Z, et al. Characterization of the prognostic and oncologic values of ITGB superfamily members in pancreatic cancer. *J Cell Mol Med*. 2020;24(22):13481–13493.
26. Yang W, Tanaka Y, Bundo M, et al. Antioxidant signaling involving the microtubule motor KIF12 is an intracellular target of nutrition excess in beta cells. *Dev Cell*. 2014;31(2):202–214.
27. Jin S, Song C, Jia S, et al. An integrated strategy for establishment of curcuminoid profile in turmeric using two LC-MS/MS platforms. *J Pharm Biomed Anal*. 2017;132:93–102.
28. Xiang X, Song C, Shi Q, et al. A novel predict-verify strategy for targeted metabolomics: comparison of the curcuminoids between crude and fermented turmeric. *Food Chem*. 2020;331, 127281.
29. Chen YN, Hsu SL, Liao MY, et al. Ameliorative effect of curcumin-encapsulated hyaluronic acid-PLA nanoparticles on thioacetamide-induced murine hepatic fibrosis. *Int J Environ Res Publ Health*. 2016;14(1):11.
30. Yan X, Yu X, Jiang C, et al. Tonifying-Qi-and-Detoxification Decoction attenuated injuries of colon and lung tissues in ulcerative colitis rat model via regulating NF-kappaB and p38MAPK pathway. *Ann Transl Med*. 2022;10(8):455.
31. Sun Q, Li L, Zhou Q. Effects of ethanolic extract of Schisandra sphenanthera on the pharmacokinetics of rosuvastatin in rats. *Drug Des Dev Ther*. 2022;16:1473–1481.
32. Xu W, Xiao M, Li J, et al. Hepatoprotective effects of Di Wu Yang Gan: a medicinal food against CCl(4)-induced hepatotoxicity in vivo and in vitro. *Food Chem*. 2020;327, 127093.
33. Zhang FP, Huang YP, Luo WX, et al. Construction of a risk score prognosis model based on hepatocellular carcinoma microenvironment. *World J Gastroenterol*. 2020;26(2):134–153.
34. Zhuang H, Cao G, Kou C, et al. CCL2/CCR2 axis induces hepatocellular carcinoma invasion and epithelial-mesenchymal transition in vitro through activation of the Hedgehog pathway. *Oncol Rep*. 2018;39(1):21–30.
35. Zhi Y, Lu H, Duan Y, et al. Involvement of the nuclear factor-kappaB signaling pathway in the regulation of CXC chemokine receptor-4 expression in neuroblastoma cells induced by tumor necrosis factor-alpha. *Int J Mol Med*. 2015;35(2):349–357.
36. Mecca C, Giambanco I, Donato R, et al. Microglia and aging: the role of the TREM2-DAP12 and cx3cl1-cx3cr1 axes. *Int J Mol Sci*. 2018;19(1).
37. Zhang M, Liu HL, Huang K, et al. Fuzheng huayu recipe prevented and treated CCl4-induced mice liver fibrosis through regulating polarization and chemotaxis of intrahepatic macrophages via CCL2 and CX3CL1. *Evid Based Complement Alternat Med*. 2020;2020, 8591892.
38. Cao N, Chen T, Guo ZP, et al. Monoammonium glycyrrhizate suppresses tumor necrosis factor-alpha induced chemokine production in HMEC-1 cells, possibly by blocking the translocation of nuclear factor-kappaB into the nucleus. *Can J Physiol Pharmacol*. 2014;92(10):859–865.
39. Zheng Y, Zhang J, Zhao Y, et al. Curcumin protects against cognitive impairments in a rat model of chronic cerebral hypoperfusion combined with diabetes mellitus by suppressing neuroinflammation, apoptosis, and pyroptosis. *Int Immunopharm*. 2021;93, 107422.
40. Xie W, Zhang H, Qin S, et al. The expression and clinical significance of secretory leukocyte proteinase inhibitor (SLPI) in mammary carcinoma using bioinformatics analysis. *Gene*. 2019;720, 144088.
41. Nugteren S, Goos J, Delis-van Diemen PM, et al. Expression of the immune modulator secretory leukocyte protease inhibitor (SLPI) in colorectal cancer liver metastases and matched primary tumors is associated with a poorer prognosis. *OncoImmunology*. 2020;9(1), 1832761.
42. Chen H, Wang H, Yu X, et al. ERCC6L promotes the progression of hepatocellular carcinoma through activating PI3K/AKT and NF-kappaB signaling pathway. *BMC Cancer*. 2020;20(1):853.
43. Gao Z, Wu J, Wu X, et al. SRPX2 boosts pancreatic cancer chemoresistance by activating PI3K/AKT axis. *Open Med*. 2020;15(1):1072–1082.
44. Jiang RH, Xu JJ, Zhu DC, et al. Glycyrrhizin inhibits osteoarthritis development through suppressing the PI3K/AKT/NF-kappaB signaling pathway in vivo and in vitro. *Food Funct*. 2020;11(3):2126–2136.
45. Zhou Y, Zhang M, Zhang Z, et al. Hydrazinocurcumin and 5-fluorouracil enhance apoptosis and restrain tumorigenicity of HepG2 cells via disrupting the PTEN-mediated PI3K/Akt signaling pathway. *Biomed Pharmacother*. 2020;129, 109851.
46. Yan H, Jung KH, Kim J, et al. Artemisia capillaris extract AC68 induces apoptosis of hepatocellular carcinoma by blocking the PI3K/AKT pathway. *Biomed Pharmacother*. 2018;98:134–141.

47. Jin D, Cao M, Mu X, et al. Catalpol inhibited the proliferation of T24 human bladder cancer cells by inducing apoptosis through the blockade of akt-mediated anti-apoptotic signaling. *Cell Biochem Biophys*. 2015;71(3):1349–1356.
48. Zhang Z, Yang L, Hou J, et al. Molecular mechanisms underlying the anticancer activities of licorice flavonoids. *J Ethnopharmacol*. 2021;267, 113635.
49. Zhou J, Dong Y, Liu J, et al. AQP5 regulates the proliferation and differentiation of epidermal stem cells in skin aging. *Braz J Med Biol Res*. 2020;53(11), e10009.
50. Chen L, Xiao D, Tang F, et al. CAPN6 in disease: an emerging therapeutic target. *Int J Mol Med*. 2020;46(5):1644–1652.
51. Hong X, Hong X, Zhao H, et al. Knockdown of SRPX2 inhibits the proliferation, migration, and invasion of prostate cancer cells through the PI3K/Akt/mTOR signaling pathway. *J Biochem Mol Toxicol*. 2018, e22237.
52. Cui X, Liu X, Han Q, et al. DPEP1 is a direct target of miR-193a-5p and promotes hepatoblastoma progression by PI3K/Akt/mTOR pathway. *Cell Death Dis*. 2019;10 (10):701.
53. Zhou Q, Lui VW, Yeo W. Targeting the PI3K/Akt/mTOR pathway in hepatocellular carcinoma. *Future Oncol*. 2011;7(10):1149–1167.
54. Iozzo RV, Sanderson RD. Proteoglycans in cancer biology, tumour microenvironment and angiogenesis. *J Cell Mol Med*. 2011;15(5):1013–1031.
55. Luo C, Shibata K, Suzuki S, et al. GPC3 expression in mouse ovarian cancer induces GPC3specific T cell-mediated immune response through M1 macrophages and suppresses tumor growth. *Oncol Rep*. 2014;32(3):913–921.
56. Pan Z, Chen C, Long H, et al. Overexpression of GPC3 inhibits hepatocellular carcinoma cell proliferation and invasion through induction of apoptosis. *Mol Med Rep*. 2013;7(3):969–974.
57. Moroz A, Wang YH, Sharib JM, et al. Theranostic targeting of CUB domain containing protein 1 (CDCP1) in pancreatic cancer. *Clin Cancer Res*. 2020;26(14): 3608–3615.
58. Zhao W, Yang A, Chen W, et al. Inhibition of lysyl oxidase-like 1 (LOXL1) expression arrests liver fibrosis progression in cirrhosis by reducing elastin crosslinking. *Biochim Biophys Acta, Mol Basis Dis*. 2018;1864(4 Pt A):1129–1137.
59. Xia Z, Ouyang D, Li Q, et al. The expression, functions, interactions and prognostic values of PTPRZ1: a review and bioinformatic analysis. *J Cancer*. 2019;10(7): 1663–1674.
60. Ai Y, Wu S, Zou C, et al. LINC00941 promotes oral squamous cell carcinoma progression via activating CAPRIN2 and canonical WNT/beta-catenin signaling pathway. *J Cell Mol Med*. 2020;24(18):10512–10524.
61. Capurro MI, Xiang YY, Lobe C, et al. Glypican-3 promotes the growth of hepatocellular carcinoma by stimulating canonical Wnt signaling. *Cancer Res*. 2005; 65(14):6245–6254.
62. Hu P, Ke C, Guo X, et al. Both glypican-3/Wnt/beta-catenin signaling pathway and autophagy contributed to the inhibitory effect of curcumin on hepatocellular carcinoma. *Dig Liver Dis*. 2019;51(1):120–126.
63. Zhou J, Wu N, Lin L. Curcumin suppresses apoptosis and inflammation in hypoxia/reperfusion-exposed neurons via Wnt signaling pathway. *Med Sci Mon Int Med J Exp Clin Res*. 2020;26, e920445.
64. Giannelli G, Mazzocca A, Fransvea E, et al. Inhibiting TGF-beta signaling in hepatocellular carcinoma. *Biochim Biophys Acta*. 2011;1815(2):214–223.
65. Caja L, Bertran E, Campbell J, et al. The transforming growth factor-beta (TGF-beta) mediates acquisition of a mesenchymal stem cell-like phenotype in human liver cells. *J Cell Physiol*. 2011;226(5):1214–1223.
66. Pan Z, Yang K, Wang H, et al. MFAP4 deficiency alleviates renal fibrosis through inhibition of NF-kappaB and TGF-beta/Smad signaling pathways. *Faseb J*. 2020;34 (11):14250–14263.
67. Shahid H, Shahzad M, Shabbir A, et al. Immunomodulatory and anti-inflammatory potential of curcumin for the treatment of allergic asthma: effects on expression levels of pro-inflammatory cytokines and aquaporins. *Inflammation*. 2019;42(6): 2037–2047.
68. Sun Y, Chen H, Dai J, et al. Glycyrrhizin protects mice against experimental autoimmune encephalomyelitis by inhibiting high-mobility group box 1 (HMGB1) expression and neuronal HMGB1 release. *Front Immunol*. 2018;9:1518.
69. Yang F, Hou ZF, Zhu HY, et al. Catalpol protects against pulmonary fibrosis through inhibiting TGF-beta1/smad3 and wnt/beta-catenin signaling pathways. *Front Pharmacol*. 2020;11, 594139.
70. Chen Q, Zhang H, Cao Y, et al. Schisandrin B attenuates CCl4-induced liver fibrosis in rats by regulation of Nrf2-ARE and TGF-beta/Smad signaling pathways. *Drug Des Dev Ther*. 2017;11:2179–2191.
71. Yamazaki D, Kurisu S, Takenawa T. Regulation of cancer cell motility through actin reorganization. *Cancer Sci*. 2005;96(7):379–386.
72. Yamazaki K, Takamura M, Masugi Y, et al. Adenylate cyclase-associated protein 1 overexpressed in pancreatic cancers is involved in cancer cell motility. *Lab Invest*. 2009;89(4):425–432.
73. Chen QY, Jiao DM, Yao QH, et al. Expression analysis of Cdc42 in lung cancer and modulation of its expression by curcumin in lung cancer cell lines. *Int J Oncol*. 2012; 40(5):1561–1568.